

Counter-Rotation in Disk Galaxies

E. M. Corsini

*Dipartimento di Fisica ed Astronomia ‘Galileo Galilei’, Università di Padova,
Padova, Italy*

Abstract. Counter-rotating galaxies host two components rotating in opposite directions with respect to each other. The kinematic and morphological properties of lenticulars and spirals hosting counter-rotating components are reviewed. Statistics of the counter-rotating galaxies and analysis of their stellar populations provide constraints on the formation scenarios which include both environmental and internal processes.

1. Introduction

Counter-rotating galaxies belong to the class of multi-spin galaxies. They are characterized by the presence of two components that are observed rotating in opposite directions with respect to each other. Before their discovery, counter-rotating galaxies were considered from a theoretical point of view and dismissed as elegant curiosities (see Rubin 1994b, for an historical perspective on the investigation of galactic kinematics). This belief changed when Galletta (1987) measured the kinematics of the ionized-gas and stellar components of the early-type barred galaxy NGC 4564 and showed they are rotating in opposite directions around the same rotation axis. In the same period, the first counter-rotating elliptical (NGC 5898; Bettoni 1984; Bertola & Bettoni 1988) was found in Padua too. As more and more data became available, the presence of counter-rotating components was detected in tens of galaxies along all the Hubble sequence, from ellipticals to irregulars.

Previous reviews about counter-rotation are those by Galletta (1996) and Bertola & Corsini (1999), while Corsini & Bertola (1998) listed all the counter-rotating galaxies known at the time. This paper focuses on the counter-rotation in lenticulars and spirals.

2. Varieties of the Counter-Rotating Components

The phenomenon of counter-rotation is:

- *intrinsic* when the two kinematically decoupled components are rotating in opposite directions around the same rotation axis and, therefore, their vectors of angular momentum are antiparallel;
- *apparent* if the two kinematically decoupled components rotate around skewed rotation axes and the line of sight lies in between them so that the vectors of angular momentum are projected antiparallel onto the sky plane.

Observationally, the intrinsic or apparent nature of counter-rotation may be addressed in not edge-on galaxies by analyzing their full velocity field as mapped with multi-slit or integral-field spectroscopy.

As far as the counter-rotating components are concerned, counter-rotation occurs in a variety of forms:

- *gas-versus-stars counter-rotation* (also known as *gaseous counter-rotation*) is observed when the gaseous disk counter-rotates with respect to the stellar body of the galaxy. This is the case of the SB0/SBa NGC 4546 in which the rotation of the ionized, molecular, and atomic gas ($\approx 10^8 M_\odot$) has similar amplitude but opposite direction with respect to the stars (Galletta 1987; Bettoni et al. 1991; Sage & Galletta 1994).
- *stars-versus-stars counter-rotation* (also known as *stellar counter-rotation*) occurs when two stellar components counter-rotate. Usually the more massive component is labeled as the prograde one. The E7/S0 NGC 4550 hosts two cospatial counter-rotating stellar disks, one of them is corotating with the gaseous disk (Rubin et al. 1992; Johnston et al. 2013; Coccato et al. 2013). The two stellar disks have similar luminosities, sizes, and masses (Rix et al. 1992) although one is thicker than the other (Cappellari et al. 2007). The bulge (e.g., NGC 524; Katkov et al. 2011), a secondary bar (e.g., NGC 2950; Corsini et al. 2003a; Maciejewski 2006), or some of the stars in a bar (Bettoni 1989; Bettoni & Galletta 1997) are other examples of counter-rotating stellar components.
- *gas-versus-gas counter-rotation* is reported when two gaseous disks counter-rotate. The S0 NGC 7332 possesses two apposed disks of ionized gas rotating in opposite sense with respect to each other. The gaseous material ($\approx 10^5 M_\odot$) displays non-circular motions indicating it has not reached equilibrium (Fisher et al. 1994; Plana & Boulesteix 1996).

Finally, counter-rotation in disk galaxies is detected in:

- the *inner regions* of the galaxy. For example, the Sa NGC 3593 (Fig. 1) is composed by a small bulge, a main stellar disk which contains $\sim 80\%$ of the stars ($1.2 \times 10^{10} M_\odot$) and a secondary counter-rotating stellar disk (Bertola et al. 1996; Coccato et al. 2013). The latter dominates the kinematics in the inner kpc and corotates with the disk of ionized and molecular gas (Corsini et al. 1998; García-Burillo et al. 2000).
- the *outer regions* of the galaxy. The Sab NGC 4826 (M64) contains two counter-rotating nested disks of ionized, molecular and neutral gas extending out ~ 1 and ~ 11 kpc, respectively (Braun et al. 1992, 1994; Rubin 1994a; Walterbos et al. 1994). They have similar masses ($\approx 10^8 M_\odot$) and are both coplanar to the stellar disk. Stars corotate with the inner gas. Beyond the dust lane which marks transition between the two gaseous disks, only a small fraction of stars ($\lesssim 5\%$) corotate with the outer gas (Rix et al. 1995).
- *overall the galaxy*, as for the Sa NGC 3626. This is the first spiral galaxy where the gaseous component ($\approx 10^9 M_\odot$) was observed to counter-rotate at all radii with respect to the stars (Ciri et al. 1995; García-Burillo et al. 1998; Haynes et al. 2000; Sil'chenko et al. 2010).

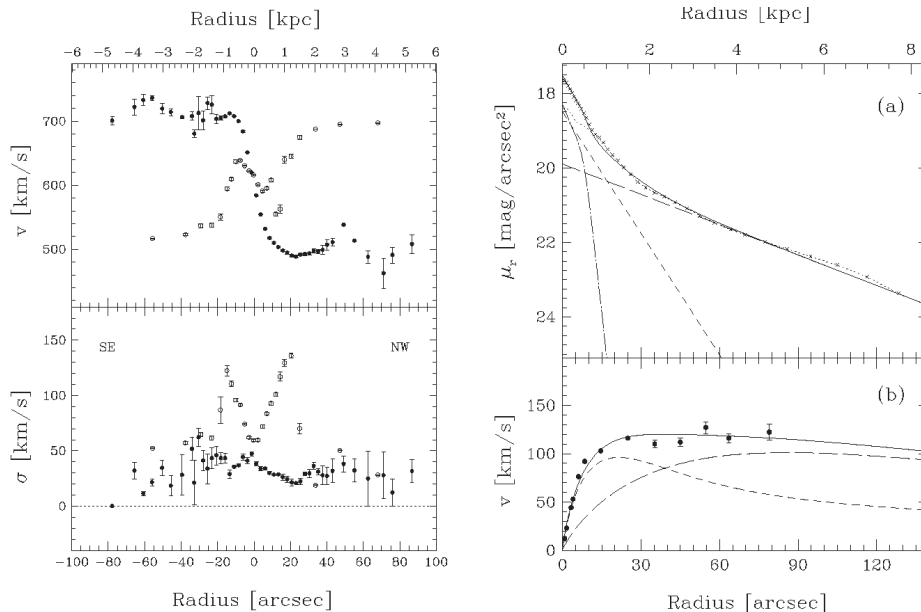


Figure 1. The inner stellar counter-rotation and overall gaseous counter-rotation of the Sa NGC 3593. Left panels: Velocity (top panel) and velocity dispersion (bottom panel) radial profiles measured along the major axis of NGC 3593 for the stellar (open circles) and ionized-gas component (filled circles). Right panels: Photometric decomposition of NGC 3593 (top panel). The surface-brightness radial profile measured along the major axis (crosses) is decomposed into the contribution of a bulge (dot-dashed line), a smaller-scale disk (short-dashed line), and a larger-scale disk (long-dashed line). The sum of the three component is given by the continuous line. Mass model of NGC 3593 (bottom panel). The contribution of the smaller-scale disk (short-dashed line) and larger-scale disk (long-dashed line) to the total circular velocity (continuous line) is shown with the observed ionized-gas velocity curve (filled circles). The contribution of the bulge is neglected. From Bertola et al. (1996).

3. Detection of Counter-Rotation

The detection of a counter-rotating gaseous component is usually straightforward. Observationally, it may be addressed by looking at the opposite orientation of the ionized-gas emission lines and stellar absorption lines in 2-dimensional optical spectra (e.g., see Fig. 1 in Galletta 1987) or in position-velocity diagrams (e.g., see Fig. 1 in Bureau & Chung 2006). Moreover, the standard techniques adopted to derive the kinematics of gas and stars allow to measure differences of few km s^{-1} in their rotation velocities.

On the contrary, unveiling a counter-rotating stellar component is a more difficult task. It requires a detailed data analysis because the kinematics of two counter-rotating stellar populations are measured from the same absorption lines. X-shaped absorption lines are only observed when the two components are photometrically similar (see Figs. 2c and 2d in Rubin et al. 1992). However, a bimodal line-of-sight velocity distribution (LOSVD) is the signature of the presence of two counter-rotating components (see Fig. 2 in Rix et al. 1992). But, the detection of the LOSVD bimodality depends on both the galaxy properties (i.e., the fraction, dynamical status, and velocity of the retro-

grade stars with respect to the prograde ones) and instrumental setup (i.e., spectral sampling and resolution) of the spectroscopic observations. By analyzing synthetic spectra with a different fraction of counter-rotating stars, Kuijken et al. (1996) and Pizzella et al. (2004) set an upper limit of $\sim 10\%$ on the fraction of retrograde stars which can be detected in long-slit spectra of intermediate resolution ($\sigma_{\text{inst}} \simeq 50 \text{ km s}^{-1}$) obtained with a spatial resolution of $\text{FWHM} \simeq 1''$ and a signal-to-noise ratio $S/N \geq 30 \text{ \AA}^{-1}$. Similar results were obtained by Coccato et al. (2013) for integral-field spectra.

The LOSVD is poorly reproduced by a Gauss-Hermite expansion (Gerhard 1993; van der Marel & Franx 1993) when the galaxy hosts a secondary kinematic component (Fabricius et al. 2012; Katkov et al. 2013). In addition, noise and aliasing features in the LOSVD can mimic what may be interpreted as a counter-rotating component. Therefore, the recovery and decomposition of parametric LOSVDs has to be performed with caution. Indeed, the counter-rotating bulge of the Sb NGC 7331 found by Prada et al. (1996) was proved by Bottema (1999) to be an artifact of the method adopted to measure the stellar kinematics. This seems also the case of the counter-rotating stellar disks of the Sb spiral NGC 7217. Fabricius et al. (in prep., but see also this volume) show that the stellar components of NGC 7217 are corotating in spite of what previously claimed by Merrifield & Kuijken (1994).

There is compelling evidence that the presence of two off-center and symmetric peaks in the stellar velocity dispersion in combination with zero velocity rotation measured along the galaxy major axis is indicative of two counter-rotating disks. This kinematic features are observed in the radial range where the two counter-rotating components have roughly the same luminosity and their LOSVDs are unresolved (Bertola et al. 1996, see Fig. 1, left panels). Recently, Krajnović et al. (2011) have found 11 galaxies (including NGC 4550) with a double-peaked velocity dispersion in the volume-limited sample of 260 nearby early-type galaxies gathered by the ATLAS-3D project. They are interesting candidates for a further investigation to address the fraction of their counter-rotating stars.

4. Environment and Morphology of Counter-Rotating Galaxies

The morphology of most of the galaxies hosting counter-rotating components appear undisturbed with no evidence of recent interaction with small satellites or companions of similar size. Indeed, the environment of counter-rotating galaxies does not appear statistically different from that of normal galaxies, as pointed out by Bettoni et al. (2001). They investigated the number, size, and distribution of the faint satellites (to a limiting magnitude $B < 21.5$) and bright companions (within a searching radius $R < 0.6 \text{ Mpc}$ and redshift difference $\Delta V < 600 \text{ km s}^{-1}$) and the large-scale environment of 49 galaxies with counter-rotation and 43 comparison galaxies without counter-rotation.

These findings set constraints on the origin of counter-rotation, because the formation process is required to not affect the present morphology of the host galaxies and the galaxy density of their surrounding regions. Therefore, retrograde gas accretion has to be a smooth and non-traumatic process, major mergers are expected to occur only early in the life of the host galaxy whereas minor mergers may be more recent. However, the relics of merger events like the collisional debris and tidal tails are generally transient and faint structures. Their surviving ages vary from a few hundred Myr to a few Gyr and they have a surface brightness that is typically $25 \text{ B-mag arcsec}^{-2}$ when

young and below $27 B\text{-mag arcsec}^{-2}$ when getting older. The detection of these fine structures requires deep optical imaging, but the comparison of their morphology and kinematics with the results of numerical simulations promises to constrain the epoch and mechanism of the second event (e.g., Corsini et al. 2002; Duc et al. 2011)

As far as the morphology of the host galaxy concerns, no counter-rotating components are detected in late-type spiral galaxies. Three of the few spirals hosting counter-rotating gaseous and/or stellar disks (NGC 3593, NGC 3626, and NGC 4138) belong to the same morphological type, being very early-type spirals (S0/a–Sa) with smooth arms. Their spiral pattern is either defined entirely or dominated by the dust lanes. Indeed, they appear in same section of the *The Carnegie Atlas of Galaxies* (Plates 72–76; Sandage & Bedke 1994). The suppression of arms in counter-rotating spirals has been recently recognized in high-resolution N-body simulations of multi-armed spiral features triggered through swing amplification by density inhomogeneities (with the mass and lifetime of the order of a typical giant molecular cloud) orbiting the disk (D’Onghia et al. 2013). A survey of a sample of early S0/a and Sa spirals selected to have the spiral pattern traced by dust lanes unveiled the presence of kinematically decoupled gas components but no new case of counter-rotation (Corsini et al. 2003b).

Previous 2-dimensional N-body simulations of disk galaxies with a significant fraction of counter-rotating stars predicted the formation of a stationary and persisting one-arm leading spiral wave (with respect to the corotating stars) due to the two-stream disk instability (Lovelace et al. 1997; Comins et al. 1997). However, the counter-rotating spirals studied so far have intermediate-to-high inclination which makes difficult to identify the presence of a one-armed spiral pattern, whereas kinematic data for low inclined one-arm systems are missing.

5. Statistics of Counter-Rotation

By analyzing the existing data of S0 galaxies for which the kinematics of the ionized gas and stellar components were measured along (at least) the major axis, Pizzella et al. (2004) found a counter-rotating (or a kinematically decoupled) gaseous component in 17/53 galaxies. This fraction corresponds to $32\%_{-11}^{+19}$ (at the 95% confidence level) and it is consistent with previous statistics by Bertola et al. (1992, 35%), Kuijken et al. (1996, $(24 \pm 8)\%$), and Kannappan & Fabricant (2001, $24\%_{-6}^{+8}$). These findings favor a scenario in which acquisition events in S0 galaxies are not limited to few peculiar objects but they are a widespread phenomenon (Bertola et al. 1992), as it is for ellipticals (Bertola et al. 1988). The recent results by Davis et al. (2011) based on integral-field spectroscopy and radio observations support this scenario too. They found that the gas in $(36 \pm 5)\%$ (40/111) of their sample of fast-rotating early-type galaxies is kinematically misaligned with respect to the stars. In addition, the ionized, molecular, and atomic gas in all the detected galaxies are always kinematically aligned, even when they are kinematically misaligned from the stars. This implies that all these phases of the interstellar medium share a common origin and underlines the role of external acquisition.

In contrast to the prevalence of counter-rotating gas in S0 galaxies, Kuijken et al. (1996) estimated that $< 10\%$ (at the 95% confidence level) of S0 galaxies host a significant fraction ($> 5\%$) of counter-rotating stars.

Pizzella et al. (2004) addressed the frequency of counter-rotation in spiral galaxies from a sample of 50 S0/a–Scd galaxies, for which the major-axis kinematics of the ionized gas and stars were obtained with the same spatial and spectral resolution, and

measured with the same analysis techniques. It turns out that $< 12\%$ and $< 8\%$ (at the 95% confidence level) of the sample galaxies host a counter-rotating gaseous and stellar disk, respectively. For comparison, Kannappan & Fabricant (2001) set an upper limit of 8% on the fraction of spirals hosting counter-rotating gas by analyzing a sample of 38 Sa–Sbc galaxies.

6. Formation Scenarios: External and Internal Processes

Numerical simulations show that episodic or prolonged accretion of gas from environment (Thakar & Ryden 1996, 1998) and merging with a gas-rich dwarf companion (Thakar & Ryden 1996; Thakar et al. 1997) are viable mechanisms for the retrograde acquisition of small amounts of external gas. They give rise to counter-rotating gaseous disks only in S0 galaxies, since in spiral galaxies the acquired gas is swept away by the pre-existing gas. Therefore, the formation of counter-rotating gaseous disks is favored in S0 galaxies since they are gas-poor systems, while spiral disks host large amounts of gas (Bettoni et al. 2003), which is corotating with the stellar component. When gas-rich systems acquire external gas in retrograde orbits, the gas clouds of the new retrograde and pre-existing prograde components collide, lose their centrifugal support, and accrete toward the galaxy center. A counter-rotating gaseous disk will be observed only if the mass of the newly supplied gas exceeds that of the pre-existing one (Lovelace & Chou 1996). A counter-rotating stellar disk is the end-result of star formation in the counter-rotating gas component. For this reason we observe a larger fraction of counter-rotating gaseous disks in S0s than in spirals (Pizzella et al. 2004). This also explains why the mass of counter-rotating gas in most S0 galaxies is small compared to that of the stellar counter-rotating components (Kuijken et al. 1996). Counter-rotating gaseous and stellar disks in spirals are both the result of retrograde acquisition of large amounts of gas, and they are observed with the same frequency (Pizzella et al. 2004). In this framework, stellar counter-rotation is the end result of star formation in a counter-rotating gaseous disk. The formation of two counter-rotating stellar disks from material accreted from two distinct filamentary structures in cosmological simulations has been recently discussed by (Algorry et al. 2014).

Usually, major mergers between disk galaxies with comparable masses are ruled out because they tend to produce ellipticals. Anyway, for a narrow range of initial conditions, major mergers are successful in building a remarkably axisymmetric disk which hosts two counter-rotating stellar components of similar mass and size (Puerari & Pfenniger 2001, see also Bettoni et al., this volume). Moreover, the coplanar merging of two counter-rotating progenitors heats more the prograde than the retrograde stellar disk and the gas ends up aligned with the total angular momentum (dominated by the orbital angular momentum), and thus with the prograde stellar disk, as observed in NGC 4550 (Crocker et al. 2009).

An alternative to the external-origin scenarios has been proposed by Evans & Collett (1994) for NGC 4550, and it involves the dissolution of a bar or a triaxial stellar halo. In this process, the stars moving on box orbits escape from the confining azimuthal potential well and move onto tube orbits. In non-rotating disks, there are as many box orbits with clockwise azimuthal motion as with counter-clockwise. Thus, half box-orbit stars are scattered onto clockwise-streaming tube orbits, half onto counter-clockwise ones. In this way, two identical counter-rotating stellar disks can be built.

Since barred galaxies host quasi-circular retrograde orbits, the origin of the stellar counter-rotation observed in barred galaxies (Bettoni 1989; Bettoni & Galletta 1997) can be the result of internal dynamical processes (Wozniak & Pfenniger 1997). Nevertheless, accreted gas can be trapped on this family of retrograde orbits and then eventually form new stars. These counter-rotating material may lead to the formation of a secondary bar rotating in opposite direction with respect to the main one (Sellwood & Merritt 1994). Observationally, the formation of secondary bars may be constrained by addressing the occurrence of counter-rotating secondary bars. Indeed, the most accepted view on the origin of secondary bars is that they form through instabilities in gas inflowing along the main bar (Shlosman et al. 1989). But, a retrograde bar is unlikely to be supported by a prograde disk. Numerical simulations suggest that two counter-rotating nested bars, formed in two counter-rotating stellar disks that overlap each other, are stable and long-living systems (Friedli 1996). This leads to the possibility that secondary bars form out of inner stellar disks, like those observed in the nuclei of several disk galaxies (Pizzella et al. 2002; Ledo et al. 2010). To date counter-rotating nuclear disks have been detected only in elliptical galaxies (e.g., Morelli et al. 2004).

7. Stellar Populations of Counter-Rotating Components

The different formation mechanisms of counter-rotating disk galaxies are expected to leave different signatures in the properties of the prograde and retrograde stellar populations. In particular, their age difference may be used to discriminate between competing scenarios for the origin of counter-rotation.

The gas accretion followed by star formation always predicts a younger age for the counter-rotating component, whereas the counter-rotating component formed by the retrograde capture of stars through minor or major mergers may be either younger or older with respect to the pre-existing stellar disk. The external origin also allows that the two counter-rotating components have different metallicities and α -enhancements. In contrast, the formation of large-scale counter-rotating stellar disks due to bar dissolution predicts the same mass, chemical composition, and age for both the prograde and retrograde components.

A spectroscopic decomposition that separates the relative contribution of the counter-rotating stellar components to the observed galaxy spectrum is therefore needed to disentangle their stellar populations. This has been recently done for the counter-rotating stellar disks of NGC 3593 (Coccatto et al. 2013), NGC 4550 (Coccatto et al. 2013; Johnston et al. 2013), and NGC 5719 (Coccatto et al. 2011). In all of them, the counter-rotating stellar disk rotates in the same direction as the ionized gas, and it is less massive, younger, more metal poor, and more α -enhanced than the main stellar disk. These findings rule out an internal origin of the secondary stellar component and favor a scenario where it formed from gas accreted on retrograde orbits from the environment fueling an *in situ* outside-in rapid star formation.

The Sab spiral NGC 5179 shows a spectacular on-going interaction with its face-on Sbc companion NGC 5713 (Fig. 2, top panel). The interaction is traced by a tidal bridge of neutral hydrogen, which feeds the counter-rotating gaseous and stellar components (Vergani et al. 2007). NGC 5719 is the first interacting disk galaxy in which counter-rotation has been detected (Fig. 2, bottom panels). The age of counter-rotating stellar population ranges from 0.7 to 2.0 Gyr and metallicity changes from subsolar ($[Z/H] \simeq -1.0$ dex) in the outskirts to supersolar ($[Z/H] \simeq 0.3$ dex) in the center,

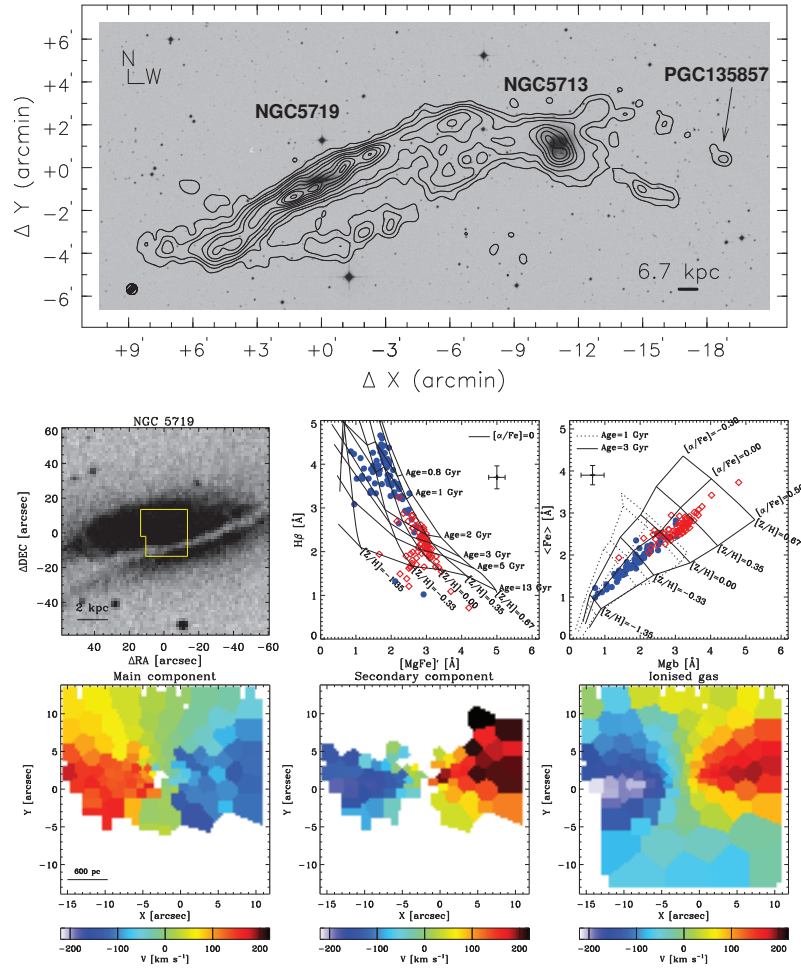


Figure 2. The counter-rotating stellar disks of the interacting Sab spiral galaxy NGC 5179. Top panels: Contour map of the H I column density distribution of NGC 5179 superimposed on an optical image from the Digitized Sky Survey. The lowest contour level is at 7.0×10^{19} atoms cm^{-2} and the increment is 2.4×10^{20} atoms cm^{-2} . From Vergani et al. (2007). Middle panels: Field of view observed with integral-field spectroscopy (left panel) and measured equivalent width of the line-strength indices H β vs. Mg b (central panel) and $\langle \text{Fe} \rangle$ vs. $[\text{MgFe}]'$ (right panel) with the predictions for age, metallicity, and α -enhancement from single stellar population models. Each spatial bin returns the indices of both the main stellar (red diamonds) and secondary counter-rotating stellar component (blue circles). From Coccato et al. (2011). Bottom panels: Two-dimensional velocity fields of the main stellar component (left panel), secondary stellar component (central panel), and ionized-gas component (right panel). From Coccato et al. (2011).

whereas the main stellar component has ages ranging from 2 to 13.5 Gyr and nearly solar metallicity. The youngest ages and highest metallicities are found in correspondence of the star forming regions. The α -enhancement of the counter-rotating component indicates a star formation history with a time-scale of 2 Gyr (Fig. 2, middle panels). On

the contrary, the formation through a major galaxy merger cannot be completely ruled out for NGC 3593 and NGC 4550, which are both quite isolated and undisturbed galaxies (Coccatto et al. 2011, 2013). A larger sample is required to understand by statistical arguments whether it was accretion or merger the most efficient mechanism to assembly counter-rotating spirals.

8. Concluding Remarks

After they were discovered three decades ago, counter-rotating galaxies still represent a challenging subject for both theorists and observers. Although the broad picture of the formation of counter-rotating galaxies is in place, we still miss many details.

A few issues should be attacked first in the near future to make a step forward in our understanding of counter-rotation in disk galaxies. They include: a deep imaging survey to look for the fingerprints of accretion and merging events in the environment of counter-rotating galaxies at very low levels of surface brightness; the analysis of a complete sample of spiral galaxies to drive unbiased conclusions about the frequency of the different kinds of counter-rotation; the derivation of the stellar LOSVD from high (spectral and spatial) resolution data obtained with wide-field integral-field units to look for yet undetected retrograde stars; and the extensive measurement of the stellar populations of the prograde and retrograde components in counter-rotating galaxies to test the predictions of the different formation scenarios.

References

- Algorry, D. G., Navarro, J. F., Abadi, M. G., et al. 2014, *MNRAS*, 437, 3596
 Bertola, F., & Bettoni, D. 1988, *ApJ*, 329, 102
 Bertola, F., Buson, L. M., & Zeilinger, W. W. 1988, *Nature*, 335, 705
 — 1992, *ApJ*, 401, L79
 Bertola, F., Cinzano, P., Corsini, E. M., et al. 1996, *ApJ*, 458, L67
 Bertola, F., & Corsini, E. M. 1999, in *IAU Symp. 186, Galaxy Interactions at Low and High Redshift*, ed. J. E. Barnes, & D. B. Sanders (Dordrecht: Kluwer), 149
 Bettoni, D. 1984, *The Messenger*, 37, 17
 Bettoni, D. 1989, *AJ*, 97, 79
 Bettoni, D., & Galletta, G. 1997, *A&AS*, 124, 61
 Bettoni, D., Galletta, G., & García-Burillo, S. 2003, *A&A*, 405, 5
 Bettoni, D., Galletta, G., & Oosterloo, T. 1991, *MNRAS*, 248, 544
 Bettoni, D., Galletta, G., & Prada, F. 2001, *A&A*, 374, 83
 Bottema, R. 1999, *A&A*, 348, 77
 Braun, R., Waltherbos, R. A. M., & Kennicutt, R. C., Jr. 1992, *Nature*, 360, 442
 Braun, R., Waltherbos, R. A. M., Kennicutt, R. C., Jr., & Tacconi, L. J. 1994, *ApJ*, 420, 558
 Bureau, M., & Chung, A. 2006, *MNRAS*, 366, 182
 Cappellari, M., Emsellem, E., Bacon, R., et al. 2007, *MNRAS*, 379, 418
 Ciri, R., Bettoni, D., & Galletta, G. 1995, *Nature*, 375, 661
 Coccatto, L., Morelli, L., Corsini, E. M., et al. 2011, *MNRAS*, 412, L113
 Coccatto, L., Morelli, L., Pizzella, A., et al. 2013, *A&A*, 549, A3
 Comins, N. F., Lovelace, R. V. E., Zeltwanger, T., & Shorey, P. 1997, *ApJ*, 484, L33
 Corsini, E. M., & Bertola, F. 1998, *J. Korean Phys. Soc.*, 33, 574
 Corsini, E. M., Debattista, V. P., & Aguerri, J. A. L. 2003a, *ApJ*, 599, L29
 Corsini, E. M., Pizzella, A., & Bertola, F. 2002, *A&A*, 382, 488
 Corsini, E. M., Pizzella, A., Coccatto, L., & Bertola, F. 2003b, *A&A*, 408, 873
 Corsini, E. M., Pizzella, A., Funes, J. G., Vega Beltran, J. C., & Bertola, F. 1998, *A&A*, 337, 80

- Crocker, A. F., Jeong, H., Komugi, S., et al. 2009, *MNRAS*, 393, 1255
 Davis, T. A., Alatalo, K., Sarzi, M., et al. 2011, *MNRAS*, 417, 882
 D’Onghia, E., Vogelsberger, M., & Hernquist, L. 2013, *ApJ*, 766, 34
 Duc, P.-A., Cuillandre, J.-C., Serra, P., et al. 2011, *MNRAS*, 417, 863
 Evans, N. W., & Collett, J. L. 1994, *ApJ*, 420, L67
 Fabricius, M. H., Saglia, R. P., Fisher, D. B., et al. 2012, *ApJ*, 754, 67
 Fisher, D., Illingworth, G., & Franx, M. 1994, *AJ*, 107, 160
 Friedli, D. 1996, *A&A*, 312, 761
 Galletta, G. 1987, *ApJ*, 318, 531
 Galletta, G. 1996, in *ASP Conf. Ser. 91, IAU Colloq. 157, Barred Galaxies*, ed. R. Buta, D. A. Crocker, & B. G. Elmegreen (San Francisco, CA: ASP), 429
 García-Burillo, S., Sempere, M. J., & Bettoni, D. 1998, *ApJ*, 502, 235
 García-Burillo, S., Sempere, M. J., Combes, F., Hunt, L. K., & Neri, R. 2000, *A&A*, 363, 869
 Gerhard, O. E. 1993, *MNRAS*, 265, 213
 Haynes, M. P., Jore, K. P., Barrett, E. A., Broeils, A. H., & Murray, B. M. 2000, *AJ*, 120, 703
 Johnston, E. J., Merrifield, M. R., Aragón-Salamanca, A., & Cappellari, M. 2013, *MNRAS*, 428, 1296
 Kannappan, S. J., & Fabricant, D. G. 2001, *AJ*, 121, 140
 Katkov, I., Chilingarian, I., Sil’chenko, O., Zasov, A., & Afanasiev, V. 2011, *Balt. Astron.*, 20, 453
 Katkov, I. Y., Sil’chenko, O. K., & Afanasiev, V. L. 2013, *ApJ*, 769, 105
 Krajnović, D., Emsellem, E., Cappellari, M., et al. 2011, *MNRAS*, 414, 2923
 Kuijken, K., Fisher, D., & Merrifield, M. R. 1996, *MNRAS*, 283, 543
 Ledo, H. R., Sarzi, M., Dotti, M., Khochar, S., & Morelli, L. 2010, *MNRAS*, 407, 969
 Lovelace, R. V. E., & Chou, T. 1996, *ApJ*, 468, L25
 Lovelace, R. V. E., Jore, K. P., & Haynes, M. P. 1997, *ApJ*, 475, 83
 Maciejewski, W. 2006, *MNRAS*, 371, 451
 Merrifield, M. R., & Kuijken, K. 1994, *ApJ*, 432, 575
 Morelli, L., Halliday, C., Corsini, E. M., et al. 2004, *MNRAS*, 354, 753
 Pizzella, A., Corsini, E. M., Morelli, L., et al. 2002, *ApJ*, 573, 131
 Pizzella, A., Corsini, E. M., Vega Beltrán, J. C., & Bertola, F. 2004, *A&A*, 424, 447
 Plana, H., & Boulesteix, J. 1996, *A&A*, 307, 391
 Prada, F., Gutierrez, C. M., Peletier, R. F., & McKeith, C. D. 1996, *ApJ*, 463, L9
 Puerari, I., & Pfenniger, D. 2001, *Ap&SS*, 276, 909
 Rix, H.-W., Franx, M., Fisher, D., & Illingworth, G. 1992, *ApJ*, 400, L5
 Rix, H.-W., Kennicutt, R. C., Jr., Braun, R., & Waltherbos, R. A. M. 1995, *ApJ*, 438, 155
 Rubin, V. C. 1994a, *AJ*, 107, 173
 — 1994b, *AJ*, 108, 456
 Rubin, V. C., Graham, J. A., & Kenney, J. D. P. 1992, *ApJ*, 394, L9
 Sage, L. J., & Galletta, G. 1994, *AJ*, 108, 1633
 Sandage, A., & Bedke, J. 1994, *The Carnegie Atlas of Galaxies* (Washington, DC: Carnegie Institution of Washington)
 Sellwood, J. A., & Merritt, D. 1994, *ApJ*, 425, 530
 Shlosman, I., Frank, J., & Begelman, M. C. 1989, *Nature*, 338, 45
 Sil’chenko, O. K., Moiseev, A. V., & Shulga, A. P. 2010, *AJ*, 140, 1462
 Thakar, A. R., & Ryden, B. S. 1996, *ApJ*, 461, 55
 — 1998, *ApJ*, 506, 93
 Thakar, A. R., Ryden, B. S., Jore, K. P., & Broeils, A. H. 1997, *ApJ*, 479, 702
 van der Marel, R. P., & Franx, M. 1993, *ApJ*, 407, 525
 Vergani, D., Pizzella, A., Corsini, et al. 2007, *A&A*, 463, 883
 Waltherbos, R. A. M., Braun, R., & Kennicutt, R. C., Jr. 1994, *AJ*, 107, 184
 Wozniak, H., & Pfenniger, D. 1997, *A&A*, 317, 14